Technical Report

Fundamental Study on Fatigue Properties of Titanium Alloys

Kenichi MORI* Hidenori TAKEBE
Shohtaroh HASHIMOTO

Abstract

This report introduces some of Nippon Steel Corporation's research on fatigue properties of the originally developed titanium alloys such as Super-TIX™ 51AF (Ti-5Al-1Fe) and Super-TIX™ 523AFM (Ti-5Al-2Fe-3Mo) used in the automobile field, and of Ti-6Al-4V widely used in the aircraft field. Since surface treatments such as inexpensive oxidation treatment are applied to automobile engine valves as wear resistance treatment, the effects of surface treatment on fatigue properties were investigated. In addition, the damage mechanism of dwell fatigue, which is the combination of room temperature creep and fatigue, and the effects of microstructural anisotropy on dwell fatigue properties were examined.

1. Introduction

Lightweight high-strength titanium alloys excellent in specific strengths at up to 500–600°C are used for the structural members, fasteners, and engine parts of aircraft, and furthermore, are used for the automobile engine parts and/or the exhaust system, and various properties such as strength, fatigue strength, fracture toughness, creep resistance, and the resistance to oxidation are required depending on the circumstances of their usages. The effects of microstructure, texture, chemical compositions, and so forth on the fatigue properties of titanium alloys have been investigated mainly for the aircraft field, and the reliability has been enhanced with the introduction of fail-safe and damage tolerant design.[1–3] Recently, the research on dwell fatigue as stated below and the research and development to consistently predict its fatigue life by utilizing the integrated computational materials engineering (ICME) are under way.[4] In Japan, in addition to aircraft, the application to automobiles, consumer products (e.g. golf club heads), and medical equipment has been developed. Therefore, in addition to the basic research on fatigue, crack propagation, and fracture toughness of titanium alloys,[5, 6] a number of researches pertaining to the properties required in the respective usage have been conducted.

Nippon Steel Corporation developed Super-TIX™ 51AF (Ti-5Al-1Fe) and Super-TIX™ 523AFM (Ti-5Al-2Fe-3Mo) with excellent strength-ductility balance by using inexpensive Fe instead of V of Ti-6Al-4V. The former is used for the connecting rod while the latter is used for the intake engine valve of automobiles. Furthermore, Super-TIX™ 10CU (Ti-1Cu) having excellent room temperature formability and high temperature strength required for the exhaust system parts has been developed, and is now being used for such parts.[7–9] This article introduces a part of the research conducted on the fatigue of titanium alloys of the Super-TIX™ series and Ti-6Al-4V.

2. Factors That Influence Fatigue Properties in the Field of Nippon Steel Titanium Alloy Usage

The highest service temperature of the automobile intake engine valve is about 350–400°C, and Ti-6Al-4V and its low-cost type alloy have been used.[10, 11] The highest service temperature of the exhaust engine valve reaches around 800°C, and the near α type alloy like Ti-6Al-2Sn-4Zr-2Mo-0.1Si having excellent creep resistance has been used. To the connecting rod, in addition to Ti-6Al-4V, the REM-added Ti-3Al-2.5V having superior machinability has been applied.[12] Furthermore, for the exhaust system parts, high temperature strength, fatigue strength, and oxidation resistance properties at 600–700°C and above are required.[13] Fatigue strength in the temperature range from room temperature to the highest service temperature is required for such applications.

With respect to the microstructure, in many cases, the intake engine valve is controlled for equiaxed microstructure that is superior in strength-ductility balance, and the exhaust engine valve that requires creep resistance is controlled for acicular microstructure. The engine valve can have a dual structure. The head portion, which requires high temperature strength, has acicular microstructure, and the stem portion, which is exposed to lower temperature, has equiaxed microstructure.[10] Furthermore, with respect to the surface treatment, in order to enhance the wear resistance of the engine valve, a hardened layer is sometimes formed by plasma carburation[10] or oxygen diffusion treatment by atmospheric heating[11]. In

* Senior Researcher, Titanium & Stainless-steel Research Dept., Materials Reliability Research Lab., Steel Research Laboratories
20-1 Shintomi, Futtsu City, Chiba Pref. 293-8511

the connecting rod, the effect on fatigue strength of the pickling to remove the oxidized layer after hot forging was considered.[14)]

Thus, the surface oxidation developed during hot processing and/or during the service in a high temperature region, and the purposely formed oxygen hardened layer exert great influence on the fatigue properties. Therefore, upon application of the originally developed alloy, in addition to the selection of the optimum material and the control of the optimum microstructure, the evaluation of the fatigue properties considering the surface character is required.

Furthermore, in the titanium alloys for aircraft, the phenomenon of the decrease of the fatigue life by dwell fatigue is recognized.[15)] That is caused by the micro texture regions (MTRs) which sometimes exceed several hundred micrometers in size, and the combination of the creep strain in the temperature range between a room temperature and about 200°C and the cyclic fatigue. These phenomena may become problematic even in other applications. Therefore, it is important to grasp the effects of the microstructure and/or the micro texture region on the damage mechanism and the fatigue life.

3. Effects of Various Factors on Fatigue Properties

3.1 Effect of heat treatment condition on fatigue properties

The effect of the heat treatment conditions on Ti-5Al-2Fe-3Mo fatigue properties is shown in **Fig. 1**.[16)] Specimens for fatigue tests were prepared from the φ13–15 mm round bar. The specimens having φ8 mm in the parallel portion were used for the annealed material and the $\alpha+\beta$ solution-treated and aged material (($\alpha+\beta$) ST + aged). For the β solution-treated and annealed material (βST + annealed), specimens having either φ6 mm (condition 4) or φ4 mm (condition 5) were used. The rotating bending fatigue tests were conducted at room temperature in air until 1×10^7 cycles were achieved.

Figure 2 shows the representative microstructures after the heat treatment. In the annealed material and the $\alpha+\beta$ solution-treated and aged material, the primary α grain size is fine and less than 10 μm, and further, in the $\alpha+\beta$ solution-treated and aged material, fine α grains are precipitated in the prior β grains. In association with these microstructures, high fatigue strength 590 MPa for the annealed material and 640–690 MPa for the $\alpha+\beta$ solution-treated and aged material were obtained at 1×10^7 cycles.

In the β solution-treated and annealed material, while the fatigue strength stays at around 490 MPa under condition 5, fatigue strength as high as 680 MPa was obtained under condition 4. Even in the β solution-treated material of which fatigue strength is generally considered to be low, in this alloy, high fatigue strength is obtained by providing appropriate heat treatment under the condition like 4, and by forming fine acicular microstructure thereby. The ratio of the fatigue strength to the tensile strength (endurance ratio) is about 0.5 in the cases of the annealed material and the $\alpha+\beta$ solution-treated and aged material. However, in the case of the β solution-treated and annealed material under condition 4, the ratio increases to about 0.6. This is considered to be attributed to multiple factors such as the disappearance of the primary α due to the β solution-treatment, the suppression of the occurrence of cracks by the growth of grain boundary α being inhibited by the relation between the chemical compositions and the cooling rate, and the suppression of the initial stage crack propagation by the fine acicular α phase precipitated in the prior β grains.

3.2 Effect of surface oxygen hardened layer on fatigue properties

The effect of the surface oxidized layer on fatigue properties was studied using the Ti-5Al-1Fe round bar (**Fig. 3**). The following specimens were prepared: for the rotating bending fatigue test: specimens having a parallel portion of φ8 mm; for the tensile test, specimens having a parallel portion of φ6.25 mm. The specimens were oxidation-treated in the air for two different treatment times, and the results were compared with untreated material. The depth of the surface oxygen hardened layer (the depth of the layer of 500 HV and above) was about 10 μm and 20 μm, respectively.

As opposed to the slight decrease from 900 MPa of the untreated material to 878 MPa of the longer-time treated material in the tensile strength, the fatigue strength decreases by about 30% from 500 MPa to 350 MPa at 1×10^7 cycles, and the endurance ratio drops from

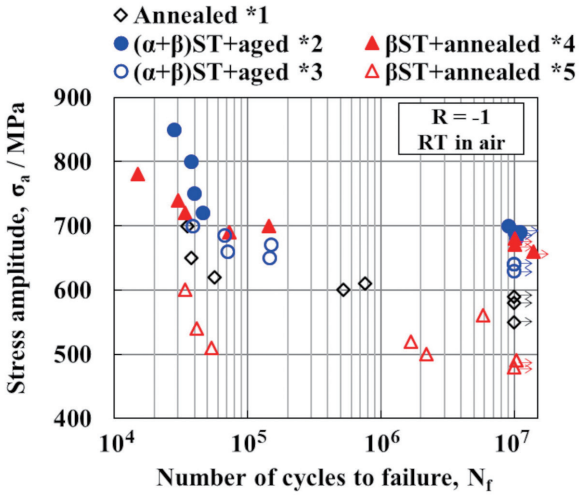

Fig. 1 Effects of heat treatment conditions for fatigue properties of Ti-5Al-2Fe-3Mo bars: Annealed (condition 1), ($\alpha+\beta$)ST and aged (condition 2 and 3), βST and annealed (condition 4 and 5)

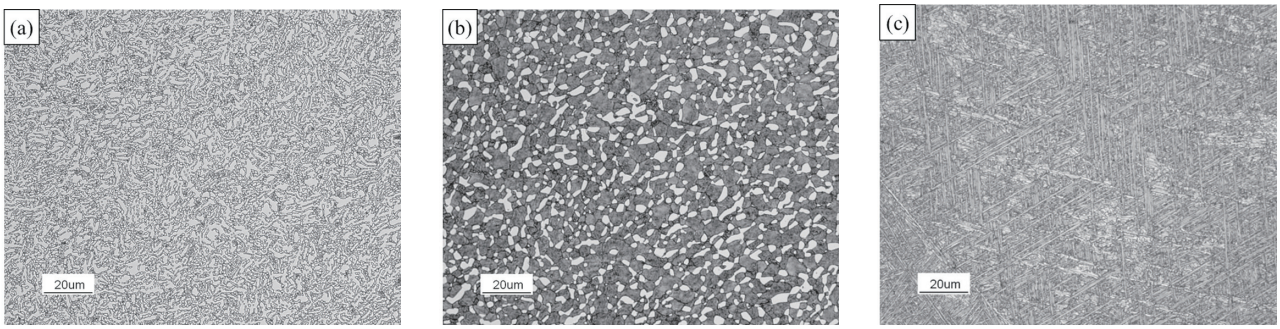

Fig. 2 Optical microstructures of Ti-5Al-2Fe-3Mo for (a) Annealed (condition 1), (b) ($\alpha+\beta$)ST and aged (condition 2), (c) βST and annealed (condition 4)

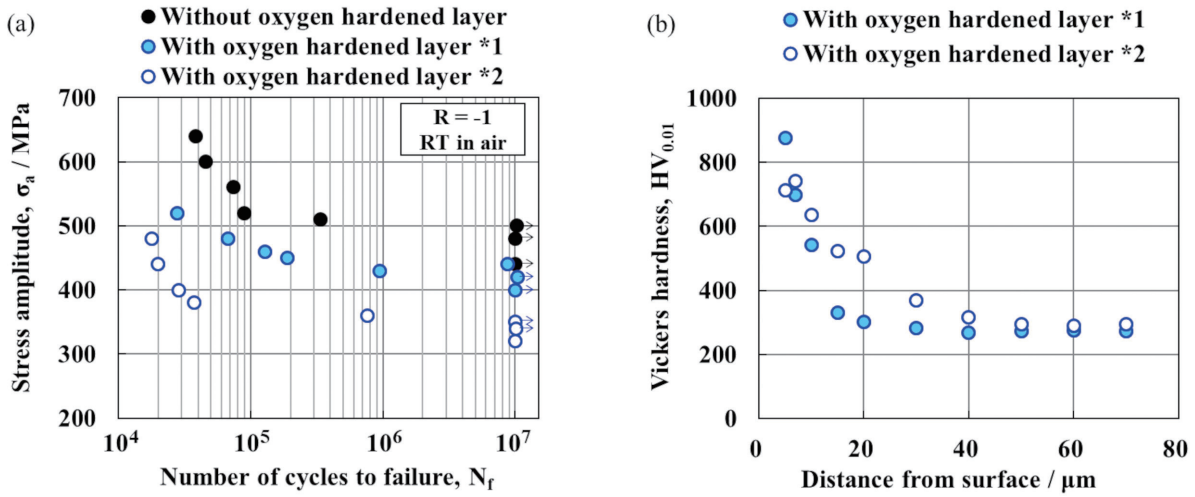

Fig. 3 (a) Effects of surface oxygen hardened layer for fatigue properties of Ti-5Al-1Fe, (b) Depth profiles of Vickers hardness of Ti-5Al-1Fe with oxygen hardened layer

0.56 to 0.40. This is considered to be attributed to the influences of the stress concentration due to the increase of the surface ruggedness and the growth of the fine cracks in the surface layer developed by the deterioration of the ductility on account of the solid solute oxygen in the surface layer.

3.3 Effect of surface treatment on fatigue properties

As described in Chapter 2, in order to give wear resistance for the application to engine valves, suppression of the stem bending due to creep deformation during inexpensive oxidation treatment is required. As stated in Section 3.1, in Ti-5Al-2Fe-3Mo, high fatigue strength is obtained with its fine acicular microstructure that is advantageous for creep resistance. Then, we studied the suppression of the deterioration of the fatigue strength while maintaining the thickness of the surface hardened layer required for wear resistance. **Figure 4** shows the result of the fatigue test conducted for Ti-5Al-2Fe-3Mo wherein the effects of the oxygen hardened layer (OHL) and the fine particle shot peening (FPB) are shown. Conditions of the solution-treatment and the oxidation treatment are the same, and even under the condition wherein the oxidized hardened layer is not formed, the heat treatment equivalent to the oxidation treatment was provided. The evaluation of the fatigue properties was conducted by the rotating bending fatigue test at room temperature in the air, using test pieces having a φ4 mm parallel portion.[16)]

Under this test condition, the fatigue strength without the oxygen hardened layer is about 640 MPa, which rises up to about 700 MPa by providing FPB treatment. On the other hand, although the fatigue strength decreases to about 390 MPa by forming the oxygen hardened layer, the fatigue strength will be recovered up to about 560 MPa by FPB treatment, and by further intensifying FPB, the fatigue strength will rise to about 700 MPa, higher than the one before the oxidation treatment. With the FPB treatment after the oxidation treatment, in addition to the effect of being provided with compressive residual stress, the effects of the disappearance of the oxidized scale layer and the reduction of the surface ruggedness are also added, and the fatigue strength is considered to be enhanced. Accordingly, an appropriate FPB treatment condition needs to be selected considering the differences in the characteristics and/or the thickness of the oxidized scale layer developed by the differences in the chemical compositions of the base material and the oxidizing condition. Furthermore, the possibility of the disappearance of the effectiveness of the compressive residual stress needs to be studied depending on the service temperature region.

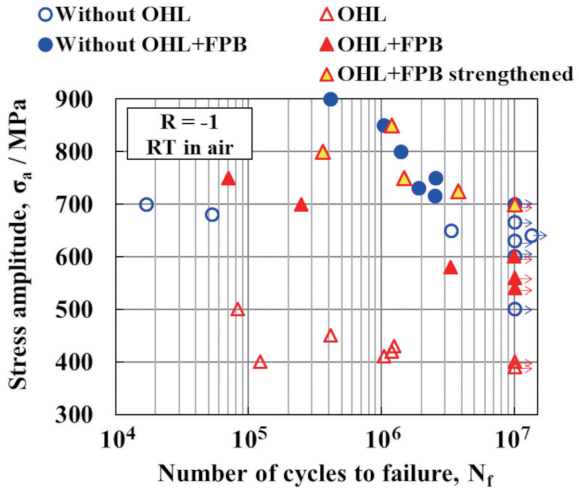

Fig. 4 Effects of oxygen hardened layer (OHL) and FPB treatment for fatigue properties of Ti-5Al-2Fe-3Mo

As another way, for example, if the wear resistance is secured by forming a CrN layer by physical vapor deposition (PVD) treatment, high fatigue strength can be achieved by the effect of avoiding the deterioration of the fatigue strength due to the oxygen hardened layer. In Ti-5Al-2Fe-3Mo, as stated in Section 3.1, by forming a CrN layer after the $\alpha+\beta$ solution-treatment, the fatigue strength can be enhanced up to about 650 MPa.

3.4 Effect of micro texture region on fatigue properties

In the $\alpha+\beta$ type titanium alloys, the microcracks in the early stage of fatigue occur on the (0001) plane of the α phase and form facets, and when the ratio of the α phase for which the (0001) plane is inclined within the range of 22° to 55° with respect to the stress axis being high, the fatigue strength deteriorates.[17)] However, even when the working temperature, working ratio, and the texture of the material are the same, there are cases in which the fatigue strength differs between those of the rolled material and the forged material. **Figure 5** shows the results of the tensile test and the axial force fa-

tigue test conducted on the test pieces taken from the rolled and forged Ti-6Al-4V bar in the longitudinal direction. The forged material shows higher fatigue strength even though the tensile strength is slightly lower as compared with those of the rolled material. A detailed study was conducted to clarify this phenomenon.[18]

Although the size of the micro texture region is larger in the rolled material, the orientation of the plane of the α phase (0001) that forms the micro texture region is different from the one wherein the microcracks are prone to occur. From the fracture surface observation, it does not appear that microcracks have occurred inside the micro texture region. Then, we considered that the microcracks occur at the boundary of the micro texture region due to the strain caused by the difference in the Young's modulus. Furthermore, the equivalent plastic strain analyzed by using the Deform 3D is larger in the forged material than that in the rolled material. Therefore, we considered that the crystal grains became more equiaxial, and the size of the micro texture region decreased in the forged material, so that the high fatigue strength is obtained.

3.5 Dwell fatigue properties and their anisotropy

The dwell fatigue damage mechanism and its anisotropy were studied by using the forged Ti-6Al-4V round bar.[19,20] In the test material, micro texture regions elongated in the longitudinal direction are formed as shown in the inverse pole figure (IPF) map of the α phase on the longitudinal cross section (**Fig. 6**). The axial force fatigue test under the stress control of the stress ratio of 0.05 was conducted by using test pieces having a φ5.08 mm parallel portion which were taken from the longitudinal and transverse directions. The fatigue loading wave forms used are the 1 s/1 s triangular wave form for the cyclic fatigue and the 1 s/120 s/1 s trapezoidal wave form for the dwell fatigue. The fatigue test results were organized with respect to the normalized value of maximum stress (σ_{max}) vs. 0.2% proof stress (normalized stress = $\sigma_{max}/\sigma_{0.2} \times 100$(%)) (**Fig. 7**). The 0.2% proof stress is 867 MPa in the longitudinal direction and 913 MPa in the transverse direction (strain rate: $8.3 \times 10^{-5}\,s^{-1}$).

When compared at the same normalized stress, the dwell fatigue life significantly decreases from the cyclic fatigue life. Furthermore, as opposed to that whereby the cyclic fatigue lives in the longitudinal direction and the transverse direction are almost the same, in the

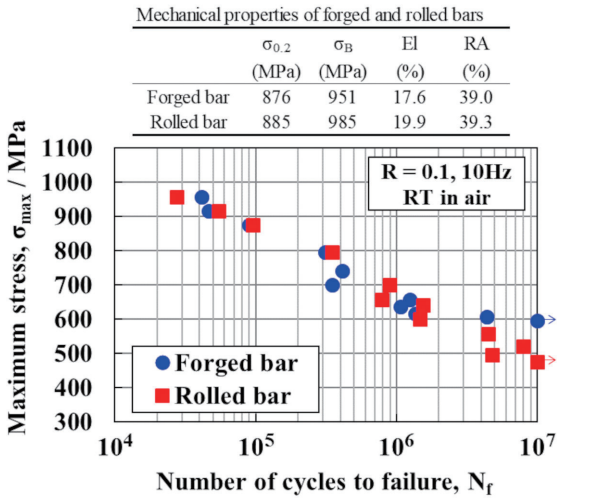

Fig. 5 Tensile and fatigue properties of forged and rolled Ti-6Al-4V bars

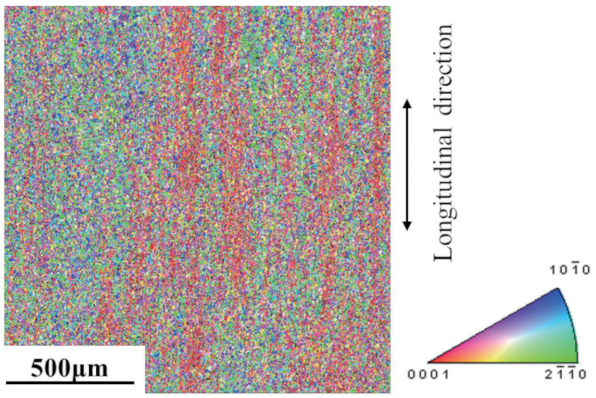

Fig. 6 IPF map for longitudinal cross section of alpha phase of Ti-6Al-4V forged bar

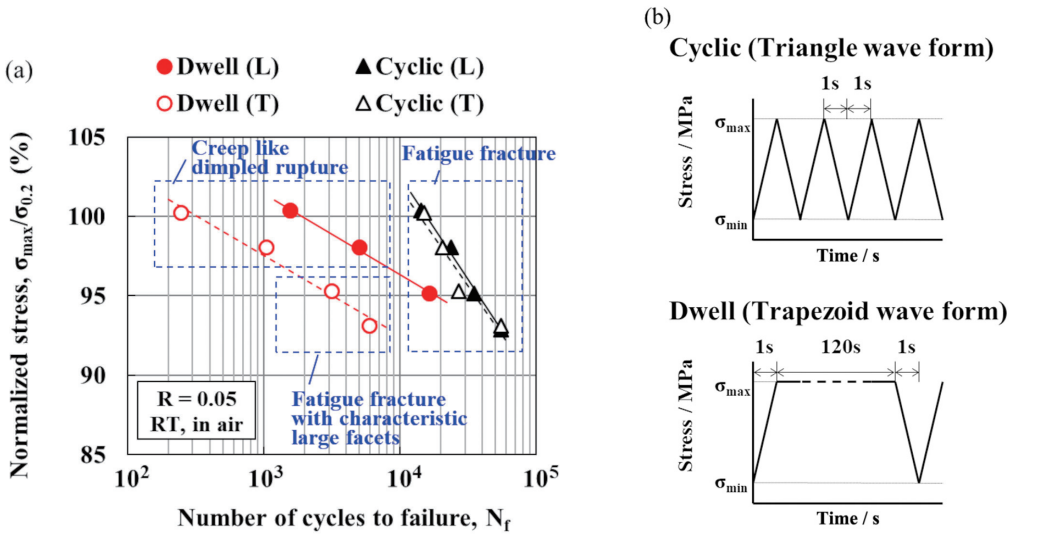

Fig. 7 (a) Relationship between ratio of maximum stress (σ_{max}) to 0.2% proof stress ($\sigma_{0.2}$) and number of cycles to failure, and classified fracture surface morphologies. (b) Fatigue loading wave forms.

dwell fatigue, the transverse direction fatigue life is about one fifth of the longitudinal direction fatigue life. In addition, in the dwell fatigue, in the high stress region of above 98% of the normalized stress (above 850 MPa in the L direction, above 895 MPa in the T direction), ductile fracture occurs in both longitudinal and transverse directions. Only in the transverse direction region below 95% of the normalized stress, the coarse facet fracture surface characterized by dwell fatigue is observed (**Fig. 8**).

Next, the relationship between the inelastic strain and the fracture life used in the analysis of the low cycle fatigue test is shown in **Fig. 9**. Herein the inelastic strain range $\Delta\varepsilon_{in}$ means the difference in the strain at unloading and loading at the mean value σ_{mean} of the maximum stress and the minimum stress. The ratchet strain ε_r means the increment of the strain right before unloading between a cycle. In the cyclic fatigue, the inelastic strain mainly consists of the plastic strain produced by the high speed stress change, and in the dwell fatigue, in addition to the plastic strain produced by the stress change, the creep strain during the stress retention period is superimposed. With respect to the data arranged in the inelastic strain range in the middle period of life, the cyclic fatigue and the dwell fatigue show different inelastic strain range $\Delta\varepsilon_{in}$ vs. fatigue life N_f relations with different inclinations. The difference in this inclination is due to the influence of the ratchet strain.

Based on the observation of the cross section of the fatigue test piece extracted during the fatigue test, we found that, in the dwell fatigue, the accumulation of strain was promoted by the ratchet strain superimposed on the increase of the inelastic strain range due to creep strain. Then the occurrence of cracks was accelerated and the number of microcracks were increased, so that the life deteriorated.

Additionally, with respect to the anisotropy of the fatigue life regarding the longitudinal direction and the transverse direction, the following is considered. In the cyclic fatigue wherein the occurrence of cracks is dominant, if the crack occurrence life is considered to be the same in the same inelastic strain range, the fatigue life in the transverse direction becomes shorter as the crack propagation rate is higher. This is supported by the result of a crack propagation test, conducted in the other research, for the same round bar. In the low ΔK region ($\Delta K \leq 15$ MPa$\sqrt{m}$), the crack propagation rate in the axial direction of the round bar is high. In the dwell fatigue, in the transverse direction, and even in the region below the 95% of normalized stress (below 870 MPa), cracks occur earlier due to the local inelastic deformation effected by the micro texture region. Furthermore, after the formation of microcracks, cracks grow rapidly, forming coarse facets along the micro texture region circumferentially, and then the fatigue life becomes short. On the other hand, in the longitudinal direction, in the region of the normalized stress below 95% (825 MPa), since the effect of creep is small, and the micro texture region in the direction of the propagation of cracks is small, along with the lowering of the maximum stress, the change from the ductile fracture to the conventional fatigue fracture occurred. So that, coarse facet is not formed on the fracture surface.

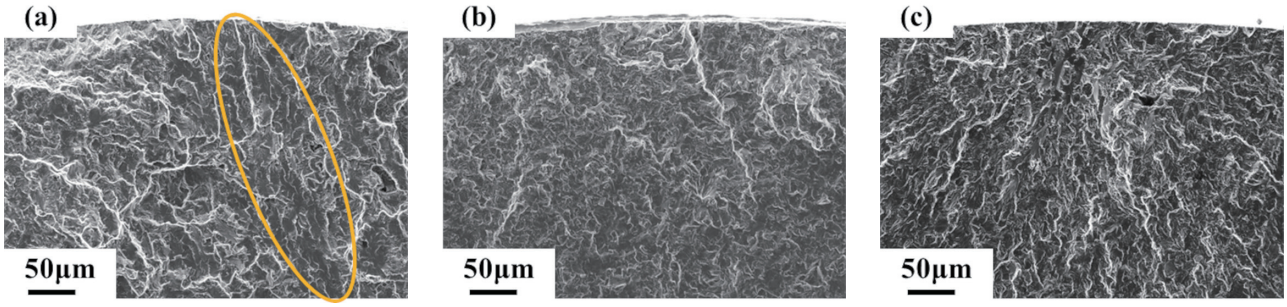

Fig. 8 SEM images of fracture surface for (a) dwell fatigue (T), (b) dwell fatigue (L), (c) cyclic fatigue (T) at σ_{max}=95% of $\sigma_{0.2}$

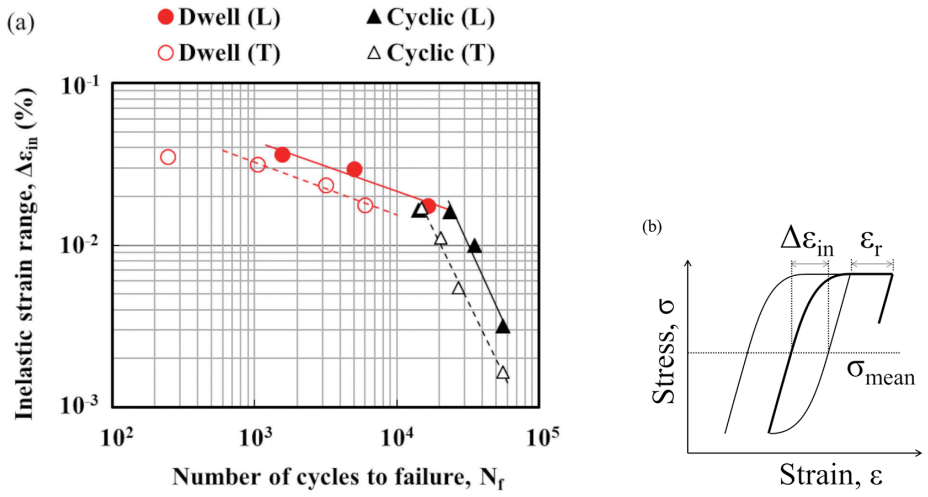

Fig. 9 (a) Relationship between inelastic strain range and number of cycles to failure, (b) Schematic diagram of stress-strain hysteresis loop showing inelastic strain range ($\Delta\varepsilon_{in}$) and ratchet strain (ε_r)

4. Conclusion

Demand for higher strength and weight reduction of structural material not only of titanium alloys is growing more sophisticated, and along with it, securing of reliability by enhancing the fatigue strength and the fracture toughness is also an important subject. We consider that hereafter, the application of computational technologies such as analytical technology like EBSD and the crystalline plasticity analysis for the clarification of the fatigue and fracture phenomena will further advance, the result of which will be further reflected in the material microstructure control and in enhancing the efficiency in constructing the guideline for the process design. The development of materials and process technologies realized by these R&Ds is expected to contribute to the solution of social problems.

References

1) Lütjering, G., Williams, J.C.: Titanium. 2nd edition. 2007, p.203–216
2) Nishikiori, S.: Journal of Japan Institute of Light Metals. 55 (11), 557 (2005)
3) Toi, Y.: Bulletin of the Society of Naval Architects of Japan. 766, 246 (1993)
4) Venkatesh, V. et al.: The 14th World Conference on Titanium (Ti-2019), MATEC Web of Conferences 321, 11091 (2020)
5) Kobayashi, T. et al.: Journal of the Society of Materials Science, Japan. 36, 831 (1987)
6) Niinomi, M. et al.: Journal of Japan Institute of Light Metals. 42 (11), 605 (1992)
7) Fujii, H. et al.: Nippon Steel Technical Report. (88), 70 (2003)
8) Fujii, H. et al.: Nippon Steel & Sumitomo Metal Technical Report. (106), 16 (2014)
9) Takebe, H. et al.: Nippon Steel Technical Report. (122), 181 (2019)
10) Okada, Y. et al.: Journal of Japan Foundry Engineering Society. 73 (12), 818 (2001)
11) Takahashi, K.: Journal of Japan Institute of Light Metals. 55 (12), 646 (2005)
12) Kimura, A. et al.: DENKI-SEIKO. 63 (1), 33 (1992)
13) Otsuka, H. et al.: Nippon Steel & Sumitomo Metal Technical Report. (106), 53 (2014)
14) Matsubara, T. et al.: Bulletin of the Japan Institute of Metals. 30 (5), 436 (1991)
15) Bache, M.R.: International Journal of Fatigue. 25, 1079 (2003)
16) Mori, K. et al.: Proceedings of the 12th World Conference on Titanium (Ti-2011), The Nonferrous Metals Society of China, 2012, p.2232
17) Pilchak, A.L. et al.: Proceedings of the 12th World Conference on Titanium (Ti-2011), The Nonferrous Metals Society of China, 2012, p.1007
18) Inagaki, I. et al.: Proceedings of the 13th World Conference on Titanium (Ti-2015), TMS (The Minerals, Metals & Materials Society), 2016, p.811
19) Mori, K. et al.: The 14th World Conference on Titanium (Ti-2019), MATEC Web of Conferences 321, 11025 (2020)
20) Mori, K. et al.: ISIJ International. 61 (10), 2666 (2021)

Kenichi MORI
Senior Researcher
Titanium & Stainless-steel Research Dept.
Materials Reliability Research Lab.
Steel Research Laboratories
20-1 Shintomi, Futtsu City, Chiba Pref. 293-8511

Hidenori TAKEBE
Senior Researcher
Titanium & Stainless-steel Research Dept.
Materials Reliability Research Lab.
Steel Research Laboratories

Shohtaroh HASHIMOTO
Titanium & Stainless-steel Research Dept.
Materials Reliability Research Lab.
Steel Research Laboratories